

A Method to Polarize Stored Antiprotons to a High Degree

F. Rathmann^{1,*}, P. Lenisa², E. Steffens³, M. Contalbrigo², P.F. Dalpiaz², A. Kacharava³, A. Lehrach¹, B. Lorentz¹, R. Maier¹, D. Prasuhn¹, and H. Ströher¹

¹ *Institut für Kernphysik, Forschungszentrum Jülich, 52428 Jülich, Germany*

² *Università di Ferrara and INFN, 44100 Ferrara, Italy and*

³ *Physikalisches Institut II, Universität Erlangen-Nürnberg, 91058 Erlangen, Germany*

(Dated: October 2, 2018)

Polarized antiprotons can be produced in a storage ring by spin-dependent interaction in a purely electron-polarized hydrogen gas target. The polarizing process is based on spin transfer from the polarized electrons of the target atoms to the orbiting antiprotons. After spin filtering for about two beam lifetimes at energies $T \approx 40 - 170$ MeV using a dedicated large acceptance ring, the antiproton beam polarization would reach $P = 0.2 - 0.4$. Polarized antiprotons would open new and unique research opportunities for spin-physics experiments in $\bar{p}p$ interactions.

PACS numbers: 29.27.Hj, 24.70.+s, 29.25.Pj

For more than two decades, physicists have tried to produce beams of polarized antiprotons. Conventional methods like atomic beam sources (ABS), appropriate for the production of polarized protons and heavy ions cannot be applied, since antiprotons annihilate with matter. Polarized antiprotons have been produced from the decay in flight of $\bar{\Lambda}$ hyperons at Fermilab. The achieved intensities with antiproton polarizations $P > 0.35$ never exceeded $1.5 \cdot 10^5 \text{ s}^{-1}$ [1]. Scattering of antiprotons off a liquid hydrogen target could yield polarizations of $P \approx 0.2$, with beam intensities of up to $2 \cdot 10^3 \text{ s}^{-1}$ [2]. Unfortunately, both approaches do not allow efficient accumulation in a storage ring, which would greatly enhance the luminosity. Spin splitting using the Stern-Gerlach separation of the given magnetic substates in a stored antiproton beam was proposed in 1985 [3]. Although the theoretical understanding has much improved since then [4], spin splitting using a stored beam has yet to be observed experimentally.

Interest in the polarization of antiprotons has recently been stimulated by a proposal to build a High Energy Storage Ring (HESR) for antiprotons at the new Facility for Antiproton and Ion Research (FAIR) at the Gesellschaft für Schwerionenforschung (GSI) in Darmstadt [5]. A Letter-of-Intent for spin-physics experiments has been submitted by the PAX collaboration [6] to employ a polarized antiproton beam incident on a polarized internal storage cell target [7]. A beam of polarized antiprotons would enable new experiments, such as the first direct measurement of the transversity distribution of the valence quarks in the proton, a test of the predicted opposite sign of the Sivers-function — related to the quark distribution inside a transversely polarized nucleon — in Drell-Yan as compared to semi-inclusive deep-inelastic scattering, and a first measurement of the moduli and the relative phase of the time-like electric and magnetic form factors $G_{E,M}$ of the proton [6].

In 1992 an experiment at the Test Storage Ring (TSR) at MPI Heidelberg showed that an initially unpolarized

stored 23 MeV proton beam can be polarized by spin-dependent interaction with a polarized hydrogen gas target [8, 9, 10]. In the presence of polarized protons of magnetic quantum number $m = \frac{1}{2}$ in the target, beam protons with $m = \frac{1}{2}$ are scattered less often, than those with $m = -\frac{1}{2}$, which eventually caused the stored beam to acquire a polarization parallel to the proton spin of the hydrogen atoms during spin filtering. In an analysis by Meyer three different mechanisms were identified, that add up to the measured result [11]. One of these mechanisms is spin transfer from the polarized electrons of the hydrogen gas target to the circulating protons. Horowitz and Meyer derived the spin transfer cross section $p + \vec{e} \rightarrow \vec{p} + e$ (using $c = \hbar = 1$) [12],

$$\sigma_{e||} = -\frac{4\pi\alpha^2(1+a)m_e}{p^2m_p} \cdot C_0^2 \cdot \frac{v}{2\alpha} \cdot \sin\left(\frac{2\alpha}{v} \ln(2pa_0)\right), \quad (1)$$

where α is the fine-structure constant, a is the anomalous magnetic moment of the proton, m_e and m_p are the rest mass of electron and proton, p is the momentum in the CM system, $a_0 = 52900 \text{ fm}$ is the Bohr radius and $C_0^2 = 2\pi\eta/[\exp(2\pi\eta) - 1]$ is the square of the Coulomb wave function at the origin. The Coulomb parameter η is given by $\eta = -z\alpha/v$ (for antiprotons, η is positive). z is the beam charge number and v the relative velocity of particle and projectile in the laboratory system.

In the following we evaluate a concept for a dedicated antiproton polarizer ring (AP). Antiprotons would be polarized by the spin-dependent interaction in an electron-polarized hydrogen gas target. This spin-transfer process is *calculable*, whereas, due to the absence of polarized antiproton beams in the past, a measurement of the spin-dependent $\bar{p}p$ interaction is still lacking, and only theoretical models exist [13]. The polarized antiprotons would be subsequently transferred to an experimental storage ring (ESR) for measurements (Fig. 1). Both the AP and the ESR should be operated as synchrotrons with electron cooling to counteract emittance growth. In both rings the beam polarization should be

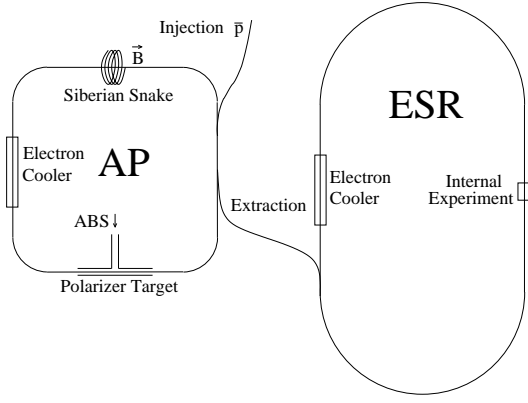


FIG. 1: Antiproton polarizer (AP) and experimental storage ring (ESR).

preserved during acceleration without loss [14]. The longitudinal spin-transfer cross section is twice as large as the transverse one [11], $\sigma_{e\parallel} = 2 \cdot \sigma_{e\perp}$, the stable spin direction of the beam at the location of the polarizing target should therefore be longitudinal as well, which requires a Siberian snake in a straight section opposite the polarizing target [15].

A hydrogen gas target of suitable substate population represents a dense target of quasi-free electrons of high polarization and areal density. Such a target can be produced by injection of two hyperfine states with magnetic quantum numbers $|m_J = +\frac{1}{2}, m_I = +\frac{1}{2}\rangle$ and $|+\frac{1}{2}, -\frac{1}{2}\rangle$ into a strong longitudinal magnetic holding field of about $B_{\parallel} = 300$ mT. The maximum electron and nuclear target polarizations in such a field are $Q_e = 0.993$ and $Q_z = 0.007$ [16]. Polarized atomic beam sources presently produce a flux of hydrogen atoms of about $q = 1.2 \cdot 10^{17}$ atoms/s in two hyperfine states [17]. Our model calculation for the polarization buildup assumes a moderate improvement of 20%, i.e. a flow of $q = 1.5 \cdot 10^{17}$ atoms/s.

The beam lifetime in the AP can be expressed as function of the Coulomb-Loss cross section $\Delta\sigma_C$ and the total hadronic $\bar{p}p$ cross section σ_{tot} ,

$$\tau_{\text{AP}} = \frac{1}{(\Delta\sigma_C + \sigma_{\text{tot}}) \cdot d_t \cdot f_{\text{AP}}} . \quad (2)$$

The density d_t of a storage cell target depends on the flow of atoms q into the feeding tube of the cell, its length along the beam L_{beam} , and the total conductance C_{tot} of the storage cell $d_t = \frac{1}{2} \frac{L_{\text{beam}} \cdot q}{C_{\text{tot}}}$ [7]. The conductance of a cylindrical tube C_o for a gas of mass M in the regime of molecular flow (mean free path large compared to the dimensions of the tube) as function of its length L , diameter d , and temperature T , is given by $C_o = 3.8 \cdot \sqrt{\frac{T}{M}} \cdot \frac{d^3}{L + \frac{4}{3}d}$. The total conductance C_{tot} of the storage cell is given by $C_{\text{tot}} = C_o^{\text{feed}} + 2 \cdot C_o^{\text{beam}}$, where C_o^{feed} denotes the conductance of the feeding tube

circumference of AP	L_{AP}	150 m
β -function at target	β	0.2 m
radius of vacuum chamber	r	5 cm
gap height of magnets	$2g$	14 cm
ABS flow into feeding tube	q	$1.5 \cdot 10^{17}$ atoms/s
storage cell length	L_{beam}	40 cm
feeding tube diameter	d_{feed}	1 cm
feeding tube length	L_{feed}	15 cm
longitudinal holding field	B_{\parallel}	300 mT
electron polarization	Q_e	0.9
cell temperature	T	100 K

TABLE I: Parameters of the AP and the polarizing target section.

and C_o^{beam} the conductance of one half of the beam tube. The diameter of the beam tube of the storage cell should match the ring acceptance angle Ψ_{acc} at the target, $d_{\text{beam}} = 2 \cdot \Psi_{\text{acc}} \cdot \beta$, where for the β -function at the target, we use $\beta = \frac{1}{2} L_{\text{beam}}$. One can express the target density in terms of the ring acceptance, $d_t \equiv d_t(\Psi_{\text{acc}})$, where the other parameters used in the calculation are listed in Table I.

The Coulomb-loss cross section $\Delta\sigma_C$ (using $c = \hbar = 1$) can be derived analytically in terms of the square of the total energy s by integration of the Rutherford cross section, taking into account that only those particles are lost that undergo scattering at angles larger than Ψ_{acc} ,

$$\Delta\sigma_C(\Psi_{\text{acc}}) = 4\pi\alpha^2 \frac{(s - 2m_p^2)^2 4m_p^2}{s^2(s - 4m_p^2)^2} \left(\frac{1}{\Psi_{\text{acc}}^2} - \frac{s}{4m_p^2} \right) . \quad (3)$$

The total hadronic cross section is parameterized using a function inversely proportional to the Lorentz parameter β_{lab} . Based on the $\bar{p}p$ data [18] the parameterization

$$\sigma_{\text{tot}} = \frac{75.5}{\beta_{\text{lab}}} \text{ (mb)} \quad (4)$$

yields a description of σ_{tot} with $\approx 15\%$ accuracy up to $T \approx 1000$ MeV. The AP revolution frequency is given by

$$f_{\text{AP}} = \frac{\beta_{\text{lab}} \cdot c}{L_{\text{AP}}} . \quad (5)$$

The resulting beam lifetime in the AP as function of the kinetic energy T is depicted in Fig. 2 for different acceptance angles Ψ_{acc} .

The buildup of polarization due to the spin-dependent $\bar{p}e$ interaction in the target [Eq. (1)] as function of time t is described by

$$P(t) = \tanh\left(\frac{t}{\tau_p}\right) , \text{ where } \tau_p = \frac{1}{\sigma_{e\parallel} d_t f_{\text{AP}} Q_e} \quad (6)$$

denotes the polarization buildup time. The time dependence of the beam intensity is described by

$$I(t) = I_0 \cdot \exp\left(-\frac{t}{\tau_{\text{AP}}}\right) \cdot \cosh\left(\frac{t}{\tau_p}\right) , \quad (7)$$

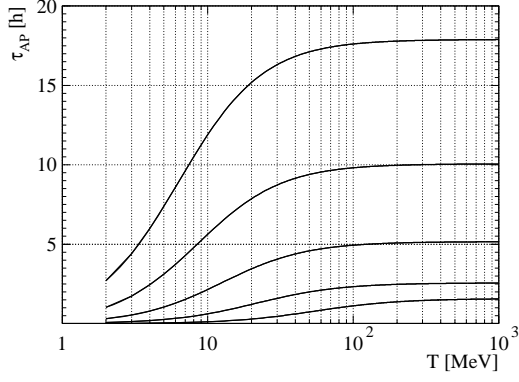


FIG. 2: Beam lifetime in the AP as function of kinetic energy T . From top to bottom the lines denote $\Psi_{\text{acc}} = 50, 40, 30, 20$, and 10 mrad.

where $I_0 = N_{\bar{p}}^{\text{AP}} \cdot f_{\text{AP}}$.

The quality of the polarized antiproton beam can be expressed in terms of the *Figure of Merit* [19]

$$\text{FOM}(t) = P(t)^2 \cdot I(t). \quad (8)$$

The optimum interaction time t_{opt} , where $\text{FOM}(t)$ reaches the maximum, is given by $\frac{d}{dt}\text{FOM}(t) = 0$. For the situation discussed here, $t_{\text{opt}} = 2 \cdot \tau_{\text{AP}}$ constitutes a good approximation that deviates from the true values by at most 3%. The magnitude of the antiproton beam polarization $P(t_{\text{opt}})$ based on electron spin transfer [Eq. (6)] is depicted in Fig. 3 as function of beam energy T for different acceptance angles Ψ_{acc} .

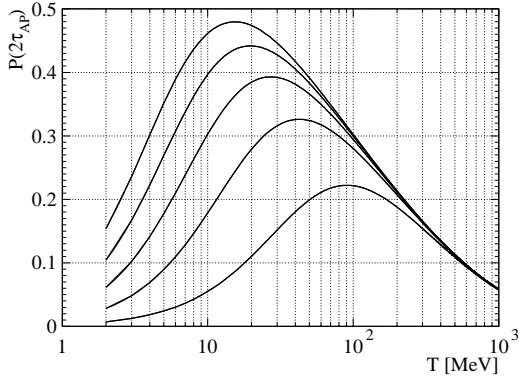


FIG. 3: Antiproton beam polarization $P(2 \cdot \tau_{\text{AP}})$ [Eq. (6)] as function of beam energy for different acceptance angles Ψ_{acc} . (Lines are organized as in Fig. 2.)

The number of antiprotons stored in the AP may be limited by space-charge effects. With an antiproton production rate of $R = 10^7 \bar{p}/s$, the number of antiprotons available at the beginning of the filtering procedure corresponds to

$$N_{\bar{p}}^{\text{AP}}(t=0) = R \cdot 2 \cdot \tau_{\text{AP}}. \quad (9)$$

The individual particle limit in the AP is given by [20]

$$N_{\text{ind.}} = 2 \pi \varepsilon \beta_{\text{lab}}^2 \gamma_{\text{lab}}^3 (r_p F)^{-1} \Delta Q, \quad (10)$$

where $\varepsilon = \Psi_{\text{acc}}^2 \cdot \beta$ denotes the vertical and horizontal beam emittance, β_{lab} and γ_{lab} are the Lorentz parameters, $r_p = 1.5347 \cdot 10^{-18}$ m is the classical proton radius, and $\Delta Q = 0.01$ is the allowed incoherent tune spread. The form factor F for a circular vacuum chamber [20] is given by $F = 1 + \left(a_y \cdot \frac{a_x + a_y}{r^2}\right) \cdot \varepsilon_2 \cdot (\gamma_{\text{lab}}^2 - 1) \cdot \frac{r^2}{g^2}$, where the mean semi-minor horizontal (x) and vertical (y) beam axes $a_{x,y} = \sqrt{\varepsilon \cdot \beta_{x,y}}$ are calculated from the mean horizontal and vertical β -functions $\beta_{x,y} = L_{\text{AP}} \cdot (2\pi\nu)^{-1}$ for a betatron-tune $\nu = 3.6$. For a circular vacuum chamber and straight magnet pole pieces the image force coefficient $\varepsilon_2 = 0.411$. The parameter r denotes the radius of the vacuum chamber and g half of the height of the magnet gaps (Table I).

The optimum beam energies for different acceptance angles at which the polarization buildup works best, however, cannot be obtained from the maxima in Fig. 3. In order to find these energies, one has to evaluate at which beam energies the FOM [Eq. (8)], depicted in Fig. 4, reaches a maximum. The optimum beam energies for polarization buildup in the AP are listed in Table II. The limitations due to space-charge, $N_{\bar{p}}^{\text{AP}} > N_{\text{ind.}}$ [Eqs. (9, 10)], are visible as kinks in Fig. 4 for the acceptance angles $\Psi_{\text{acc}} = 40$ and 50 mrad, however, the optimum energies are not affected by space-charge.

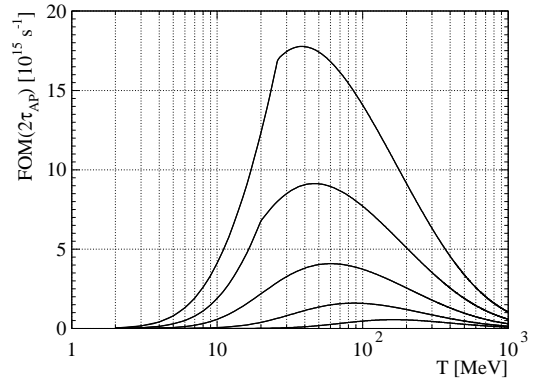


FIG. 4: Figure of Merit for the polarized antiproton beam for filtering times $t = 2 \cdot \tau_{\text{AP}}$ as function of beam energy. The parameters associated with the maxima are summarized in Table II. (Lines are organized as in Fig. 2.)

Spin filtering in a *pure* electron target greatly reduces the beam losses, because σ_{tot} disappears and Coulomb scattering angles in $\bar{p}e$ collisions do not exceed Ψ_{acc} of any storage ring. With stationary electrons stored in a Penning trap, densities of about 10^{12} electrons/cm² may be reached in the future [21]. A typical electron cooler operated at 10 kV with polarized electrons of intensity ≈ 1 mA ($I_e \approx 6.2 \cdot 10^{15}$ electrons/s) [22],

Ψ_{acc} (mrad)	T (MeV)	τ_{AP} (h)	$P(2\tau_{\text{AP}})$
10	167	1.2	0.19
20	88	2.2	0.29
30	61	4.6	0.35
40	47	9.2	0.39
50	39	16.7	0.42

TABLE II: Kinetic beam energies where the polarized antiproton beam in the AP reaches the maximum FOM for different acceptance angles.

$A = 1 \text{ cm}^2$ cross section, and $l = 5 \text{ m}$ length reaches $d_t = I_e \cdot l \cdot (\beta_{\text{lab}} c A)^{-1} = 5.2 \cdot 10^8 \text{ electrons/cm}^2$, which is six orders of magnitude short of the electron densities achievable with a neutral hydrogen gas target. For a pure electron target the spin transfer cross section is $\sigma_{e||} = 670 \text{ mb}$ (at $T = 6.2 \text{ MeV}$) [12], about a factor 15 larger than the cross sections associated to the optimum energies using a gas target (Table II). One can therefore conclude that with present day technologies, both above discussed alternatives are no match for spin filtering using a polarized gas target.

In order to estimate the luminosities available for the ESR, we use the parameters of the HESR ($L_{\text{HESR}} = 440 \text{ m}$). After spin filtering in the AP for $t_{\text{opt}} = 2 \cdot \tau_{\text{AP}}$, the number of polarized antiprotons transferred to HESR is $N_{\bar{p}}^{\text{AP}}(t = 0)/e^2$ [Eq. (9)]. The beam lifetime in the HESR at $T = 15 \text{ GeV}$ for an internal polarized hydrogen gas target of $d_t = 7 \cdot 10^{14} \text{ cm}^{-2}$ is about $\tau_{\text{HESR}} = 12 \text{ h}$ [Eqs. (2, 5)], where the target parameters from Table I were used, a cell diameter $d_{\text{beam}} = 0.8 \text{ cm}$, and $\sigma_{\text{tot}} = 50 \text{ mb}$. Subsequent transfers from the AP to the HESR can be employed to accumulate antiprotons. Eventually, since τ_{HESR} is finite, the average number of antiprotons reaches equilibrium, $\bar{N}_{\bar{p}}^{\text{HESR}} = R/e^2 \cdot \tau_{\text{HESR}} = 5.6 \cdot 10^{10}$, independent of τ_{AP} . An average luminosity of $\bar{\mathcal{L}} = R/(e^2 \cdot \sigma_{\text{tot}}) = 2.7 \cdot 10^{31} \text{ cm}^{-2}\text{s}^{-1}$ can be achieved, with antiproton beam polarizations depending on the AP acceptance angle Ψ_{acc} (Table II).

We have shown that with a dedicated large acceptance antiproton polarizer ring ($\Psi_{\text{acc}} = 10$ to 50 mrad), beam polarizations of $P = 0.2$ to 0.4 could be reached. The energies at which the polarization buildup works best range from $T = 40$ to 170 MeV . In equilibrium, the average luminosity for double-polarization experiments in an experimental storage ring (e.g. HESR) after subsequent transfers from the AP could reach $\bar{\mathcal{L}} = 2.7 \cdot 10^{31} \text{ cm}^{-2}\text{s}^{-1}$.

The antiproton polarizer, discussed here, would provide highly polarized antiproton beams of unprecedented quality. In particular the implementation of this option at the Facility for Antiproton and Ion Research would open new and unique research opportunities for spin-physics experiments in $\bar{p}p$ interactions at the HESR.

We would like to thank J. Haidenbauer and N.N. Niko-

laev for many insightful discussions on the subject.

* Electronic address: f.rathmann@fz-juelich.de

- [1] D.P. Grosnick *et al.*, Nucl. Instrum. Methods **A290**, 269 (1990).
- [2] H. Spinka *et al.*, *Proc. of the 8th Int. Symp. on Polarization Phenomena in Nuclear Physics*, Bloomington, Indiana, 1994, Eds. E.J. Stephenson and S.E. Vigdor, AIP Conf. Proc. **339** (AIP, Woodbury, NY, 1995), p. 713.
- [3] T.O. Niinikoski and R. Rossmanith, Nucl. Instrum. Methods **A255**, 460 (1987).
- [4] P. Cameron *et al.*, *Proc. of the 15th Int. Spin Physics Symp.*, Upton, New York, 2002, Eds. Y.I. Makdisi, A.U. Luccio, and W.W. MacKay, AIP Conf. Proc. **675** (AIP, Melville, NY, 2003), p. 781.
- [5] Conceptual Design Report for *An International Facility for Antiproton and Ion Research*. Available from www.gsi.de/GSI-Future/cdr.
- [6] *Antiproton-Proton Scattering Experiments with Polarization*, Letter-of-Intent for the HESR at FAIR, Jülich (2004), Spokespersons: P. Lenisa and F. Rathmann, and references therein. Available from www.fz-juelich.de/ikp/pax.
- [7] E. Steffens and W. Haeberli, Rep. Prog. Phys. **66**, 1887 (2003).
- [8] F. Rathmann *et al.*, Phys. Rev. Lett. **71**, 1379 (1993).
- [9] K. Zapfe *et al.*, Rev. Sci. Instrum. **66**, 28 (1995).
- [10] K. Zapfe *et al.*, Nucl. Instrum. Methods **A368**, 627 (1996).
- [11] H.O. Meyer, Phys. Rev. **E50**, 1485 (1994).
- [12] C.J. Horowitz and H.O. Meyer, Phys. Rev. Lett. **72**, 3981 (1994).
- [13] V. Mull and K. Holinde, Phys. Rev. **C 51**, 2360 (1995).
- [14] Preservation of beam polarization is routinely accomplished at COSY-Jülich [23], and at higher energies at the AGS of BNL [24].
- [15] Ya. S. Derbenev *et al.*, Part. Accel. **8**, 115 (1978); A. Lehrach and R. Maier, *Proc. of the 2001 Particle Accelerator Conference*, Chicago, Illinois, 2001, Eds. P. Lucas and S. Webber, (IEEE, Piscataway, NJ, 2001), p. 2566.
- [16] W. Haeberli, Ann. Rev. Nucl. Sci. **17**, 373 (1967).
- [17] A. Zelenski *et al.*, Nucl. Instrum. Methods **A**, in press, available from www.sciencedirect.com/science/article/B6TJM-4D97J59-3/2/fa6
- [18] Particle Data Group, available from pdg.lbl.gov/2002.
- [19] G.G. Ohlsen and P.W. Keaton, Nucl. Instrum. Methods **109**, 41 (1973).
- [20] C. Bovet *et al.*, A Selection of Formulae and Data useful for the design of A.G. Synchrotrons, CERN/MPS-SI/Int. DL/70/4, 23 April (1970).
- [21] J.H. Malmberg *et al.*, *Non-neutral Plasma Physics*, Eds. C.W. Roberson and C.F. Driscoll, (AIP, New York, 1988), p. 28.
- [22] J. Grames *et al.*, see p. 1047 of ref [4].
- [23] A. Lehrach *et al.*, see p. 153 of ref [4].
- [24] F.Z. Khiari *et al.*, Phys. Rev. **D 39**, 45 (1989); H. Huang *et al.*, Phys. Rev. Lett. **73**, 2982 (1994); M. Bai *et al.*, Phys. Rev. Lett. **80**, 4673 (1998).